WELDING RESEARCH

SUPPLEMENT TO THE *WELDING JOURNAL*, OCTOBER 2001
Sponsored by the American Welding Society and the Welding Research Council.

Simulation of Dynamic Behavior in a GMAW System

A model is developed to predict variations in welding parameters due to surface tension and electromagnetic force

BY J. H. CHOI, J. Y. LEE, AND C. D. YOO

ABSTRACT. The dynamic behavior of a GMAW system is simulated using a short circuiting transfer model incorporated with characteristic equations for the power supply, welding wire, and arc. The wire equation, which relates the variation of the wire extension to the wire feed and melting rates, is modified to include the effect of a molten drop attached at the wire tip. With this modification, the behavior of the GMAW system is described more precisely, and information about the initial bridge volume is provided to simulate the short circuit transfer.

A short circuit model is proposed to predict the variation of short circuit parameters considering the effects of surface tension and electromagnetic force due to current. Variation of welding parameters are continuously simulated during short circuit as well as free-flight transfer modes, and the calculated results are in broad agreement with the experimental results that occur with argon shielding.

Introduction

Although determining the proper welding condition is an important task in the gas metal arc welding (GMAW) process, it is time consuming and requires considerable trial and error. In order to estimate the operating range of welding parameters and process stability, the behavior of the GMAW system needs to be predicted in cases of free-flight and short circuiting transfer modes. In this work, the characteristic equations for the GMAW system are solved using a simplified short circuiting transfer model to predict the dynamic behavior of the system. The simulation results are verified by comparing with the experimental results.

Since the GMAW system consists of several subsystems including the power supply, welding arc, and wire, as illustrated in Fig. 1, its characteristics depend on the dynamic behavior of each subsystem, which has been described using the characteristic equation. Ushio, *et al.* (Ref. 1), predicted the dynamic behavior of DC and pulsed GMAW by solving the characteristic equations. The power supply was converted into an equivalent RL circuit, and the wire equation was used to describe the rate change of the wire extension with respect to wire-feed and melting rates. The welding arc characteristics were expressed using Ayrton's equation modified for the gas metal arc welding globular and spray transfer modes (Refs. 1, 2). The constants for Ayrton's equation and wire melting rate were experimentally determined, and these values are used in this work for simulation. Richardson, *et al.* (Ref. 3), considered the dynamic effects of the power source on wire melting rate in pulsed GMAW. Quinn, *et al.* (Ref. 4), proposed the electrode extension model based on heat transfer to predict the variation of wire extension and to determine the welding conditions under which short circuiting transfer takes place.

In order to simulate the GMAW process continuously, it is necessary to consider the metal transfer mode. In the case of free-flight modes, such as globular and spray, the static force balance model and pinch instability theory have been most widely utilized to predict drop detaching conditions (Refs. 5, 6). However, few models were reported for the short circuit mode compared with the free-flight mode. Ishichenko (Ref. 7) proposed the simple analytic short circuit model to predict the short circuit time due to surface tension, but the effect of the electromagnetic force was ignored. Although numerical technique was recently employed to analyze the short circuit as well as the free-flight modes (Refs. 8, 9), this approach is not adequate to simulate the entire GMAW system because of its complexity and computing time. It appears that simulation of the short circuiting transfer combined with the free-flight mode has not been attempted, mainly due to lack of a proper short circuit model.

Continuous simulation of the GMAW process is of interest in this work, especially when the short circuit mode is involved, because process stability was reported to be dependent on short circuit frequency, current, and voltage signals (Refs. 10, 11). The conventional welding

KEY WORDS

GMAW
Gas Metal Arc
Short Circuiting Transfer Model
Surface Tension
Electromagnetic Force Transfer Model

J. H. CHOI, J. Y. LEE, and C. D. YOO are with the Department of Mechanical Engineering, KAIST, Yusong-gu, Taejon, Korea.

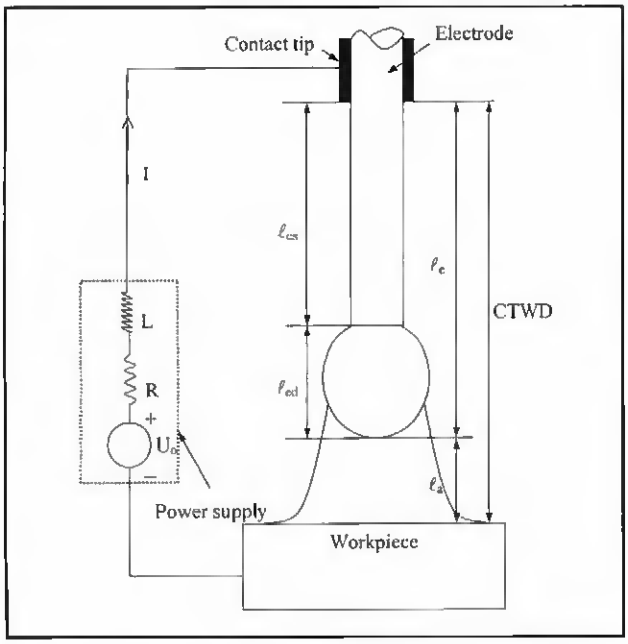

Fig. 1 — Schematic diagram of GMAW system.

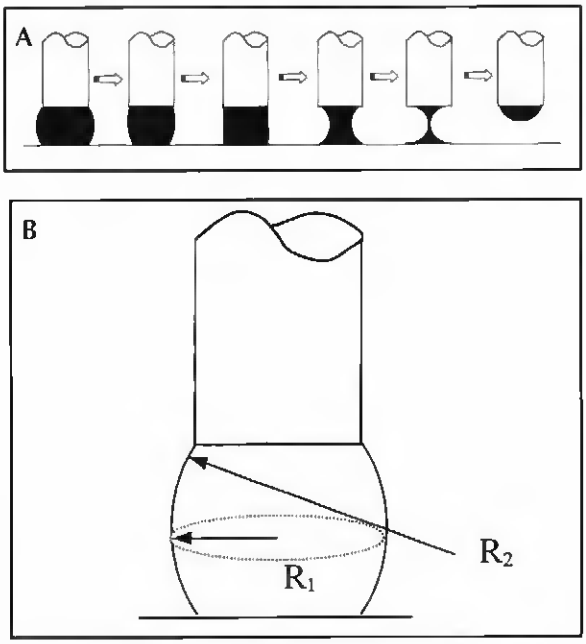

Fig. 2 — Schematics for short circuit modeling. A — Sequence of short circuiting transfer; B — bridge configuration with principal radii.

wire equation is modified to predict the system behavior more precisely and to provide the initial bridge volume for short circuiting transfer. A short circuit model is proposed to predict the variation of short circuit parameters considering the effects of surface tension and electromagnetic force. With the characteristic equations and short circuit model, it becomes possible to simulate the dynamic behavior of the GMAW system. The predicted results are compared with the experimental results for argon shielding.

Modeling of the GMAW System

Characteristic Equations

The dynamic behavior of the welding power supply, welding arc, and wire as shown in Fig. 1 is described using the corresponding characteristic equations. The power supply is converted into the equivalent RL circuit as

$$L\frac{dI}{dt} + RI = U_o - U_a \tag{1}$$

where L and R represent the inductance and resistance of the welding system, I the welding current, U_o the equivalent open-circuit voltage, and U_a the arc voltage. The welding arc characteristics are described using Ayrton's equation (Refs. 1, 2)

$$U_a = k_1 + k_2 I + (k_3 + k_4 I)\ell_a \tag{2}$$

where ℓ_a denotes the arc length and the k denotes the constants depending on the welding wire and shielding gas. The conventional wire equation has been used to describe the relationship between the rate change of the extension, wire feed, and melting rate

$$\frac{d\ell_e}{dt} = v_f - v_m \text{ and } v_m = aI + b\ell_e I^2 \tag{3}$$

where ℓ_e represents the extension, v_f the wire-feed rate, v_m the wire-melting rate, and a and b the constants for arc and joule heating, respectively.

The conventional wire equation assumes the molten portion at the wire tip is detached or removed as soon as it melts. This assumption appears to be valid in the spray mode, where small droplets are ejected at high frequency. However, in the globular mode, the molten drop grows at the wire tip for a relatively long period so that it affects the arc length and, subsequently, welding current and voltage. To predict the dynamic behavior of GMAW more precisely, the conventional wire equation needs to be modified to include the effect of a hanging droplet at the wire tip. The wire extension is described in this work as the sum of the solid extension length and molten drop length hanging at the wire tip as illustrated in Fig. 1 (*i.e.*, $\ell_e = \ell_{es} + \ell_{ed}$) so that the effect of the molten drop is considered until its detachment. In this case, the rate change of the solid wire extension depends on the wire-feed and melting rates, and the drop growth rate is proportional to the wire-melting rate until its detachment

$$\frac{d\ell_{es}}{dt} = v_f - v_m \tag{4}$$

$$\frac{dV_d}{dt} = \left(\frac{\pi D_e^2}{4}\right) v_m \tag{5}$$

where ℓ_{es} represents solid wire extension, V_d the attached drop volume, and D_e the wire diameter. The drop length, ℓ_{ed}, is calculated from the drop volume by assuming a spherical shape.

Drop detachment is determined using the force balance model and pinch instability theory for the globular and spray modes, respectively (Refs. 5, 6, 12). When the drop detaches, the entire drop volume is assumed to be ejected from the wire tip (*i.e.*, $\ell_{ed} = 0$). The short circuit transfer takes place as soon as the extension becomes equal to the contact tip to workpiece distance (CTWD). Since the arc is extinct during the short circuit period, the arc voltage in equation 1 and the constant a for arc heating in equation 3 become 0. The modified wire equation provides information about the initial bridge volume for the short circuiting transfer, as well as the effects of the hanging drop on welding parameters for the free-flight mode.

Modeling of the Short Circuiting Transfer

A short circuit model that includes the effects of surface tension and electromagnetic force is proposed and used to

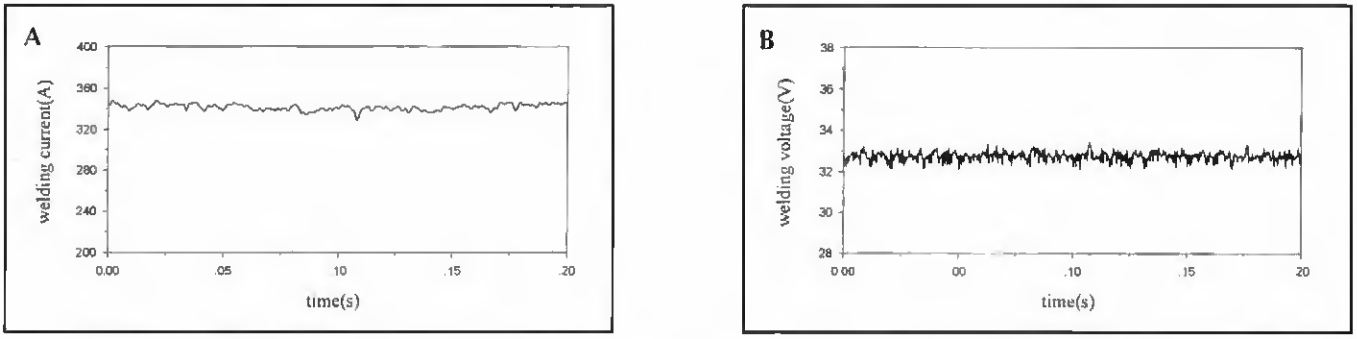

Fig. 3 — Experimental current and voltage waveforms of spray transfer. A — Current waveform; B — voltage waveform.

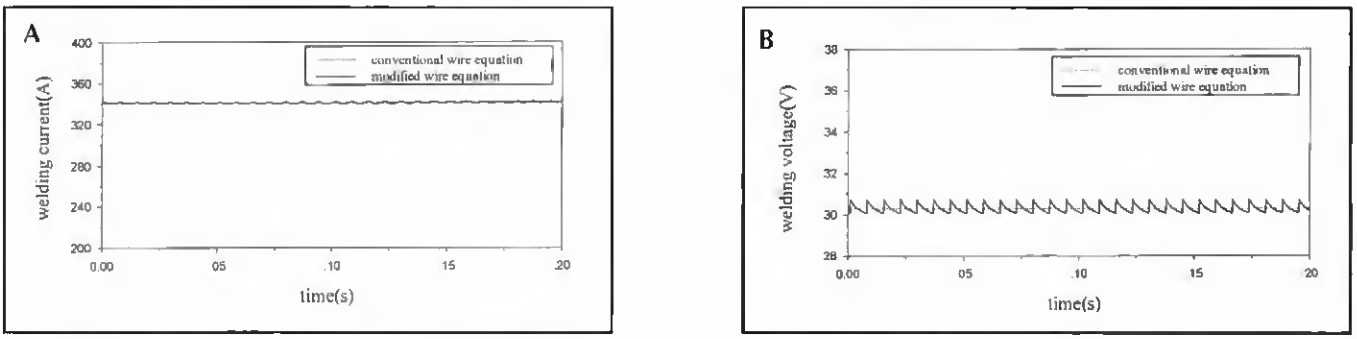

Fig. 4 — Calculated results of spray transfer using conventional and modified wire equation. A — Current waveform; B — voltage waveform.

predict variations of the welding parameters during short circuiting transfer. The following assumptions are made to simplify the complex behavior of short circuiting transfer:

1) The initial bridge shape is spherical and the contact diameter within the weld pool surface is equal to the wire diameter.

2) Flow velocity within the bridge and pressure within the weld pool are neglected.

3) The bridge shape is described by two principal radii, as illustrated in Fig. 2.

4) The pool surface remains flat and metal transfer is stable.

Once the bridge is formed, molten metal flows into the weld pool due to surface tension and electromagnetic force, and the bridge shape varies continuously as in Fig. 2A. The bridge shape is described using the principal radii of R_1 and R_2 in Fig. 2B, and R_2 is determined from the bridge volume and height, which vary continuously during a short circuit period. Given the principal radii, the average pressure on the cross section of the bridge center is derived (Ref. 12) as follows:

$$P_{avg} = \frac{\mu_0 I^2}{8\pi^2 R_1^2} + \gamma\left(\frac{1}{R_1} + \frac{1}{R_2}\right) \quad (6)$$

where μ_0 represents the permeability and γ the surface tension. Applying the Bernoulli equation with assumption 2, the flow velocity at the contact between the bridge and pool surface can be calculated using the average pressure and bridge height as

$$v = \sqrt{\frac{2}{\rho}\left(P_{avg} + \rho g h\right)} \quad (7)$$

where ρ denotes the mass density of molten metal and h the distance between the pool surface and bridge center. The volume to be transferred from the bridge to molten pool is calculated by multiplying the flow velocity, contact area, and discrete time interval Δt. The bridge volume and height are used to calculate the principal radii, and the short circuit time is the sum of the discrete time intervals until bridge breakup. It is noted that the Bernoulli equation was utilized to estimate the plasma jet velocity in the arc welding, and it predicted the experimental results within the order of magnitude (Ref. 12). Therefore, similar accuracy is expected for the flow velocity and short circuit time predicted using this short circuit model.

Calculation Procedure

When the wire-feed rate, CTWD, and equivalent open circuit voltage (OCV) are given as the inputs, variations of welding parameters such as the extension, drop volume, current, and voltage are calculated by solving the characteristic equations numerically using the Runge-Kutta method. The drop-detaching condition for the free-flight mode is determined using the force balance model and pinch instability theory. To simulate the free-flight mode, the open circuit voltage is selected to be equal to the experimental welding voltage because of the constant voltage characteristics of the GMAW power source.

When the extension becomes equal to the CTWD, the short circuit model is applied. Since the arc is extinct during the short circuit time, the effect of the arc is eliminated such that arc voltage and the constant a for arc heating in equations 1 and 3 become 0. The initial bridge volume is given from the results of characteristic equations in the free-flight mode. The pressure and flow velocity are computed using the principal radii, equations 6 and 7. Assuming constant flow velocity during the small time interval, Δt, the remaining bridge volume and corresponding principal radii are calculated for the next time step. For each time step, current and voltage are computed iteratively using equations 1 and 3, and this procedure is repeated until bridge breakup. When the arc is regenerated, effects of the arc are restored in equations 1 and 3, and half of the final bridge volume is given as the initial drop volume attached at the wire tip, as in Fig. 2A.

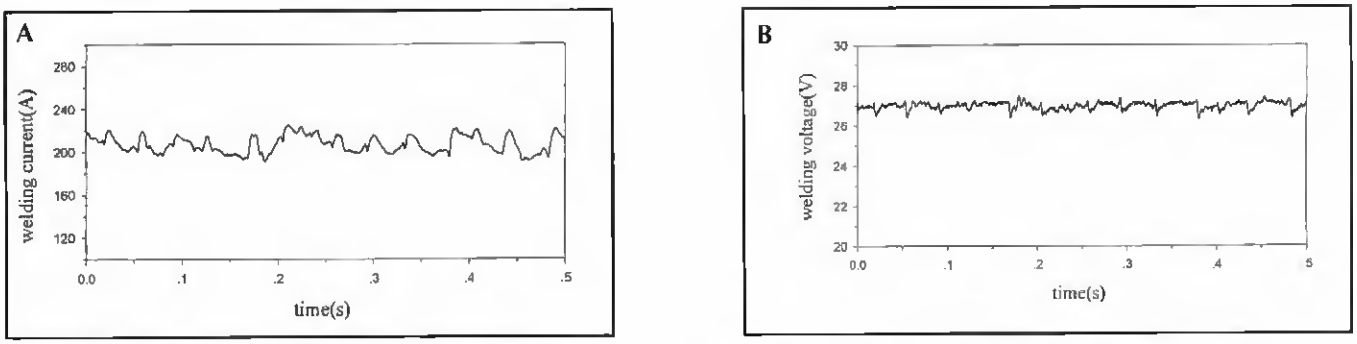

Fig. 5 — Experimental current and voltage waveforms of globular transfer. A — Current waveform; B — voltage waveform.

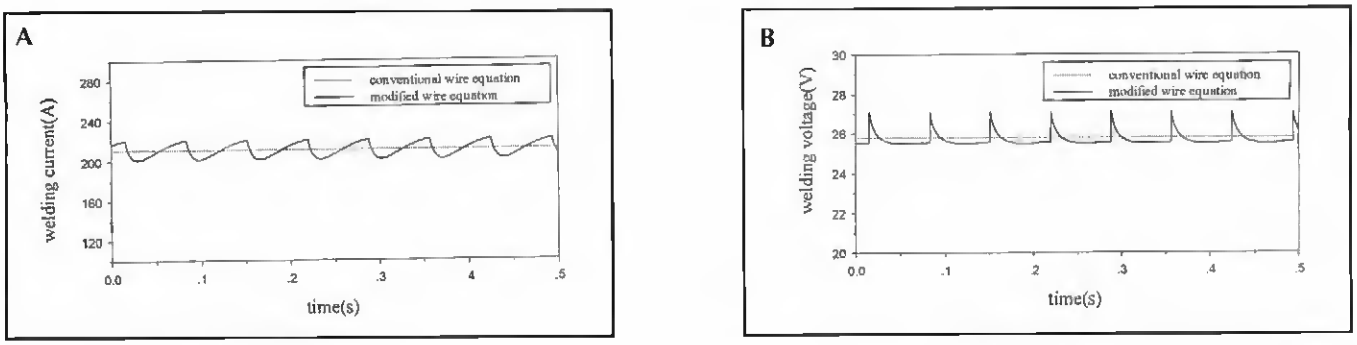

Fig. 6 — Calculated results of globular transfer using conventional and modified wire equation. A — Current waveform; B — voltage waveform.

Table 1 — Constants Used for Calculation (Refs. 1, 2)

mass density, ρ	7800 kg/m^3
kinematic viscosity, ν	2.8 x 10^{-7} m^2/s
surface tension coefficient, γ	1.2 N/m
permeability, μ_0	4π X 10^{-7} H/m
constant for arc heating, a	0.2940 mm/As (globular) 0.2383 mm/As (spray)
constant for joule heating, b	4.6081 x 10^{-5} A^{-2}s^{-1} (globular) 4.6 x 10^{-5} A^{-2}s^{-1} (spray) 6.27 x 10^{-5} A^{-2}s^{-1} (short circuit)
system resistance, R	5.0 mV/A
system inductance, L	0.35 mH
k_1	16.24 V
k_2	0.02376
k_3	0.553 V/mm
k_4	6.395 x 10^{-4}V/Amm

Results and Discussions

Globular and Spray Transfer Modes

The constants and parameters used for computation are listed in Table 1 (Refs.1, 2). It is noted that constants a, b, and each k are valid only for steel welding wire with a 1.2-mm diameter and 100% argon shielding condition. Bead-on-plate welds were made and welding parameters such as the wire-feed rate, welding current, and voltage were measured. The welding conditions were selected as CTWD of 15–25 mm, welding current of 150–350 A, and voltage of 18–34 V so that short circuit and free-flight transfer modes were produced.

Figure 3 shows the experimental results of current and voltage waveform in the spray mode under the condition of a wire-feed rate of 156.1 mm/s and CTWD of 19 mm. Average current and voltage from the experimental results are 343.2 A and 32.7 V, respectively.

The simulated results using the conventional and modified wire equations are compared in Fig. 4 where the current and voltage waveforms are calculated using the same experimental parameters and open circuit voltage (OVC) of 32.7 V. When the modified wire equation is used, small ripples caused by droplet growth and detachment are calculated in the waveform. In the case of the conventional wire equation, constant current and voltage of 340 A and 30.3 V are calculated without ripples, which correspond to the average current and voltage for the modified wire equation. In both cases, welding voltage is maintained constant with small fluctuation, which demonstrates the self-regulation effect of GMAW in the steady state. Comparing with the experimental results, the current and voltage are predicted quite accurately using the characteristic equations. The droplet at the wire tip appears to have negligible effects because small droplets are ejected at high frequency in the spray mode.

Measured current and voltage waveforms in the globular mode are shown in Fig. 5 with a wire-feed rate of 104.3 mm/s and CTWD of 25 mm. The average current and voltage of the experimental results are 207.3 A and 27 V. The calculated results using the same experimental parameters are illustrated in Fig. 6. Since the drop grows larger in the globular mode, the magnitude of the ripple increases for the modified wire equation. Similar to the spray mode, the current and voltage with the conventional wire equation are constant at 214 A and 25.9 V, respectively, which correspond to the average values with the modified wire equation. Although the effect of the attached drop increases in the globular mode, it appears to have only minor effects on welding parameters.

Short Circuiting Transfer Mode

Effects of the initial bridge volume and current on the principal radius and short

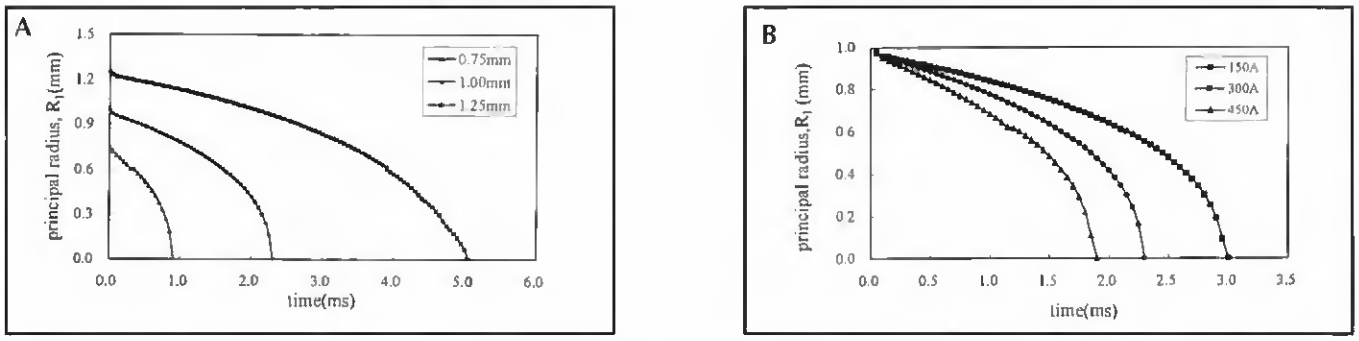

Fig. 7 — Effects of initial bridge volume and current on principal radius. A — Variation of principal radius due to initial bridge volume for constant current of 300 A; B — variation of principal radius due to constant current for initial bridge radius of 1 mm.

circuit time as predicted using the proposed short circuit model are shown in Figs. 7 and 8. The principal radius R_1 varies during the short circuit period because the bridge volume decreases continuously until bridge breakup. Variations of the principal radius, R_1, during the short circuit period are illustrated in Fig. 7. When the current is kept constant at 300 A during short circuiting transfer and imposed on the bridge with the initial bridge radius of 0.75, 1, and 1.25 mm, the short circuit time increases with larger bridge radius in Fig. 7A. When the constant currents of 150, 300, and 450 A are applied to a bridge with an initial radius of 1 mm, the short circuit time decreases with the higher current in Fig. 7B. The principal radius decreases linearly up to the wire radius of 0.6 mm, and it decays rapidly afterward because the pinch force increases due to reduction of the current-conducting area.

The effects of the initial bridge radius and current on short circuit time are illustrated in Fig. 8 where constant current is used during the short circuit period. While the short circuit time decreases with the higher current and smaller initial bridge radius, the initial bridge radius appears to have more influence on the short circuit time than the current. In practice, the relationships between the bridge volume, current, and short circuit time are coupled so that larger bridge volume induces longer short circuit time and higher current, which acts to accelerate bridge breakup. During continuous simulation, the initial bridge volume is given by solving the characteristic equations.

Figure 9 shows the experimental current and voltage waveforms in the short circuit mode with a wire-feed rate of 82.1 mm/s, welding voltage of 21.2 V and CTWD of 19 mm. Average current and voltage are 184.6 A and 18.9 V, and the short circuit frequency becomes 65.8 Hz with a short circuit and arcing time of 2.3 and 12.9 ms, respectively. The calculated results using the same experimental parameters with OCV of 21.2 V are illustrated in Fig. 10. Average current and voltage are 174 A and 20.3 V, and the short circuit frequency becomes 55 Hz with short circuit and arcing time of 1.1 and 16.9 ms. Compared with the experimental results, there exists significant discrepancy in short circuit time (2.3 vs. 1.1 ms). However, arcing time and short circuit frequency are predicted with reasonable accuracy (12.9 vs. 16.9 ms, 66 vs. 55 Hz). Since the arcing time is much longer than short circuit time, the discrepancy in short circuit time has minor effects on the frequency. While experimental peak current is higher than calculated peak current by 50 A due to longer short circuit time, the predicted average current and voltage show reasonably good agreement with the experimental results.

Since the behavior in the free-flight mode is accurately predicted, the larger discrepancy in the short circuit time appears to stem from the short circuit model. Among several reasons, assumption 2 appears to be the major cause of error because it may oversimplify the complex behavior of metal flow within the bridge and pool. Another assumption of the spherical bridge shape and

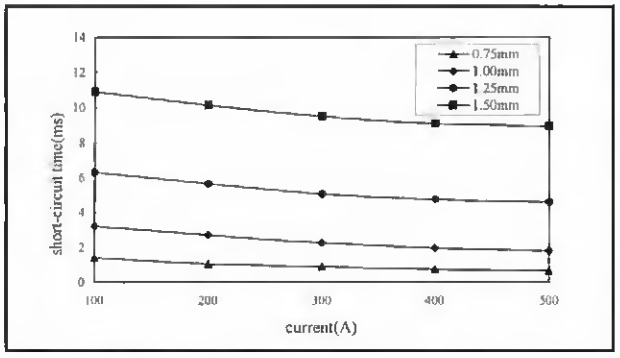

Fig. 8 — Effects of initial bridge radius and current on short circuit time.

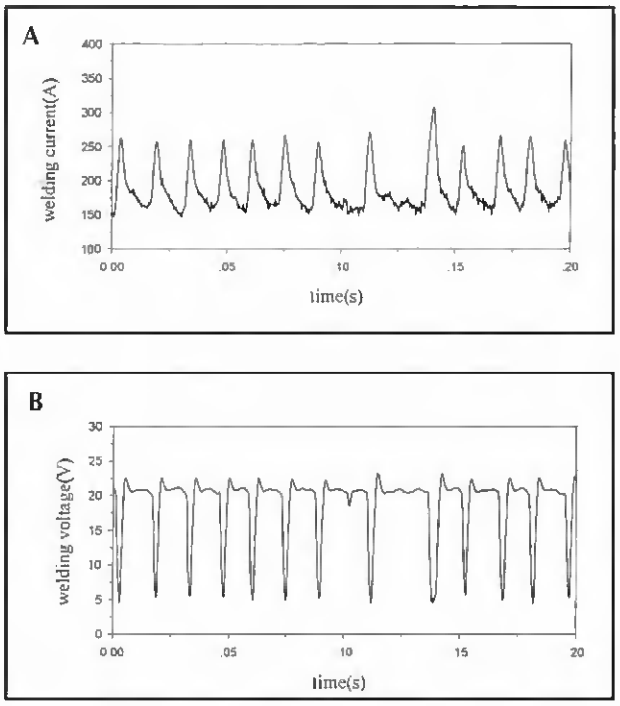

Fig. 9 — Experimental current and voltage waveforms of short circuiting transfer. A — Current waveform; B — voltage waveform.

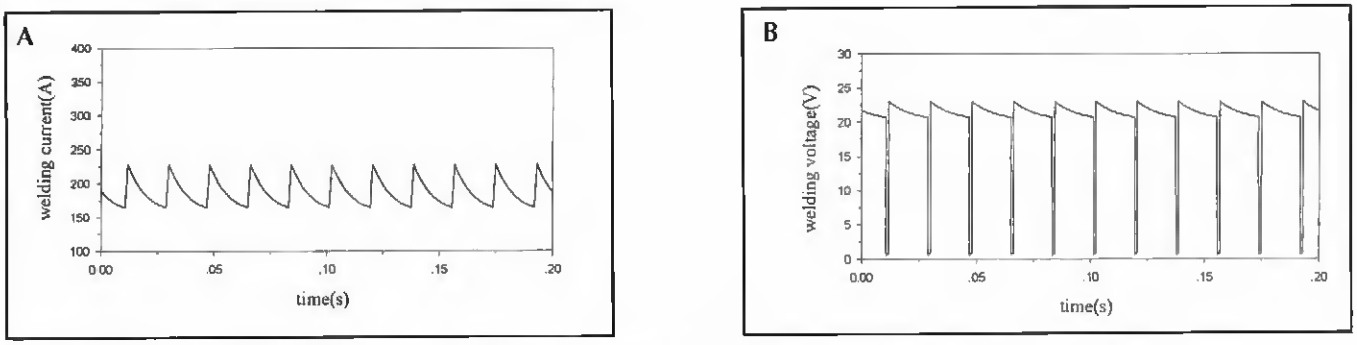

Fig. 10 — Calculated results of short circuiting transfer. A — Current waveform; B — voltage waveform.

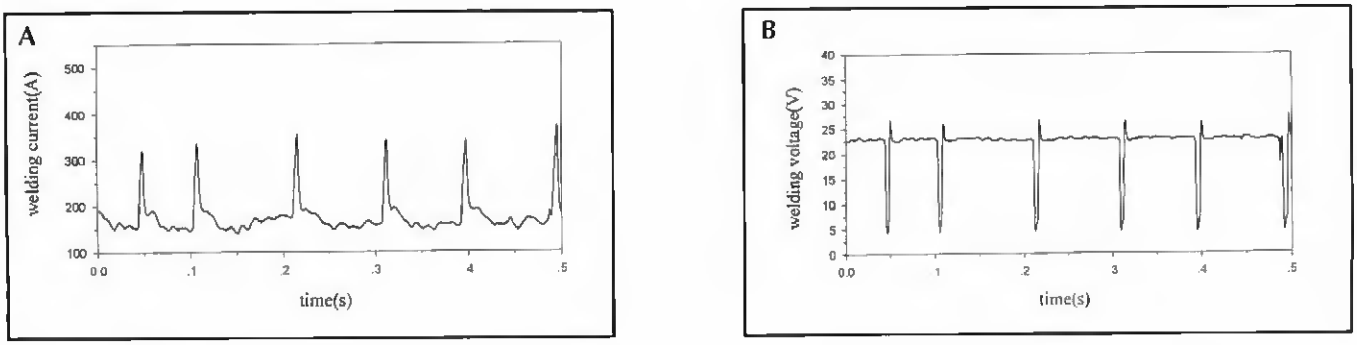

Fig.11 — Experimental current and voltage waveforms of mixed mode. A— Current waveform; B — voltage waveform.

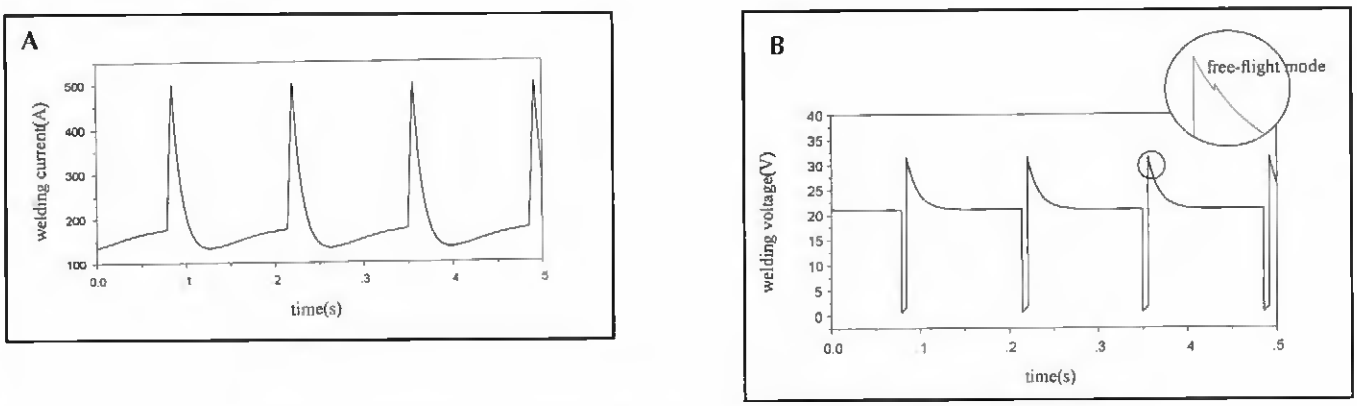

Fig. 12 — Calculated results of mixed mode. A — Current waveform; B — voltage waveform.

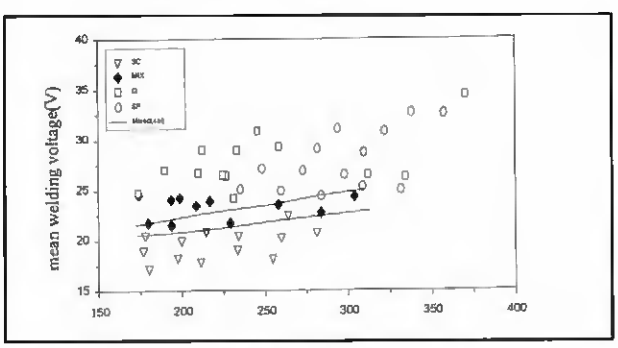

Fig. 13 — Comparison of experimental and predicted metal transfer mode.

contact condition may not be appropriate, especially when the initial bridge volume becomes smaller. Oversimplification of the proposed short circuit model includes the simple bridge shape during the short circuit period and remaining bridge volume at the bridge breakup. Further development of the short circuit model is needed for accurate prediction of the short circuit time.

Prediction of Metal Transfer Mode

A mixed metal transfer mode is calculated using the parameters at the boundary between short circuit and free-flight modes. Figure 11 shows the experimental results with the wire-feed rate of 82.1 mm/s, welding voltage of 22 V and CTWD of 19 mm. It is noted welding voltage is increased slightly higher than that in Fig. 9 (21.2 vs. 22 V). Average current and voltage are 175.7 A and 22 V, the short circuit frequency and time are 11 Hz and 4.9 ms, respectively. The simulated waveforms using the same experimental parameters with OCV of 22 V are illustrated in Fig. 12 where the average

current and voltage are 180 A and 21.1 V, and short circuit frequency and time are 13 Hz and 6.1 ms, respectively. The predicted results show reasonably good agreements with the experimental results. In addition to the short circuit mode, the drop is calculated to be detached in the free-flight mode just after bridge breakup, which demonstrates that both free-flight and short circuit modes take place in a mixed way under this welding condition.

Figure 13 shows the metal transfer modes identified using the fixed CTWD of 19 mm. The metal transfer mode including the mixed mode is predicted using the welding parameters equal to the experimental condition, and the narrow region of the mixed mode exists between the free-flight and short circuit modes. The predicted mixed and short circuit modes are in broad agreement with the experimental results. It appears the metal transfer mode as well as the variation of welding parameters can be predicted through simulation when the wire-feed rate, CTWD, and equivalent open circuit voltage are given as the inputs.

Conclusions

The dynamic behavior of the GMAW system is continuously simulated using the modified wire equation and short circuit model. Although the system behavior is predicted more precisely using the modified wire equation, it has only minor effects in the free-flight mode. The importance of the modified wire equation is to provide the initial bridge volume for the short circuit model. The short circuit model needs further improvement to yield more accurate short circuit time predictions. Combining the characteristic equations with the short circuit model, the welding current, voltage, and metal transfer mode, including the mixed mode, are predicted with reasonable accuracy for argon shielding.

Acknowledgment

The authors appreciate the financial support from the Korea Science and Engineering Foundation (No. 996-1000-002-2).

References

1. Ushio, M., and Mao, W. 1996. Modeling of the arc sensor for DC MIG/MAG welding in open arc mode — A study on the improvement of the sensitivity and the reliability of the arc sensor in GMA welding (1st report). *Journal of Japan Welding Society* 14(1): 99–107.

2. Kim, J. W., and Na, S. J. 1991. A study on prediction of welding current in GMAW. *Proc. Inst. of Mech. Engrs.* Part B 205(B1): 59–63.

3. Richardson, I. M., Bucknall, P. W., and Stares, I. 1994. The influence of power source dynamics on wire melting rate in pulsed GMAW. *Welding Journal* 73(2): 32-s to 37-s.

4. Quinn, T. P., Madigan, R. B., and Siewert, T. A. 1994. An electrode extension model for gas metal arc welding. *Welding Journal* 73(10): 241-s to 248-s.

5. Amson, J. C. 1962. An analysis of the gas shielded consumable metal arc welding system. *British Welding Journal* 62: 232–249.

6. Allum, C. J. 1985. Metal transfer in arc welding as a varicose instability: I. Varicose instability in a current-carrying liquid cylinder with surface charge. *Journal of Physics D: Applied Physics* 18: 1431–1446.

7. Ishichenko, Y. S. 1993. Relationships governing droplet transfer during a short circuit. *Welding International* 7(8): 627–631.

8. Choi, S. K., Yoo, C. D., and Kim, Y.-S. 1998. Dynamic simulation of metal transfer in GMAW — Part 1: globular and spray transfer modes. *Welding Journal* 77(1): 38-s to 44-s.

9. Choi, S. K., Ko, S. H., Yoo, C. D., and Kim, Y.-S. 1998. Dynamic simulation of metal transfer in GMAW — Part 2: short circuiting transfer mode. *Welding Journal* 77(1): 45-s to 52-s.

10. Hermans, M. J. M., and Ouden, G. den. 1999. Process behavior and stability in short circuit gas metal arc welding. *Welding Journal* 78(4): 137-s to 141-s.

11. Quinn, T. P., Smith, C., McCowan, C. N., Blachowiak, E., and Madigan, R. B. 1999. Arc sensing for defects in constant-voltage gas metal arc welding. *Welding Journal* 78(9): 322-s to 328-s.

12. Lancaster J. F. 1986. *The Physics of Welding Arc*. Pergamon Press.

Call For Papers

The two-day international conference, Supermartensitic Stainless Steels 2002, organized by the Belgian Welding Institute, is now soliciting abstracts of papers for oral presentation. The conference will be held October 3–4, 2002, in Brussels, Belgium.

The supermartensitic stainless steels are also known as the weldable martensitic stainless steels or super 13 Cr steels with low carbon content. Paper topics can include overviews, research, case histories, applications, new technology, failure reports, service experience, or anything relevant to the subject. Sales pitches promoting particular products or services will not be accepted. Main topic areas include, but are not limited to, service and applications, metallurgy, welding, fabrication, manufacturing, toughness requirements, and corrosion. The conference language will be English.

Abstracts of 300–500 words on a single A4 page should be submitted by mail, fax, or e-mail before November 1, 2001, to the Conference Secretariat. The submission should be single-line spaced, headed by the title, name(s), and affiliation(s) of all authors, along with the full address, telephone, fax, and/or e-mail of the corresponding author. Papers are accepted on the understanding the author(s) will attend the conference.

Contact information is as follows: Conference Secretariat, Marie-Anne Sorgeloos; telephone: +32 (0) 9 264 32 54; FAX: +32 (0) 9 223 73 26; e-mail: marieanne.sorgeloos@soete043.rug.ac.be. The Belgian Welding Institute, Prof. ir. A. Dhooge; telephone: +32 (0) 9 264 32 50; FAX: +32 (0) 9 223 73 26; e-mail: alfred.dhooge@rug.ac.be. Updates on the conference can be obtained from the Web site, *www.stainless-steel-world.net*.